Supplementary Table I. Select alterations associated with ERK inhibitor treatment

PDX	ERKi-sensitivity	Tumor	Alteration	Mode	Experiment
1D	Limited	LUAD	$BRAF^{amp}$	Selected	scDNA-seq, bulk-seq, FISH
1E	Limited	LUAD	$BRAF^{amp}$	Selected	bulk-seq, FISH
7	Limited	LUAD	BTK^{R46H}	Selected	bulk-seq
21	Insensitive	LUAD	$MITF^{L348F}$	De-novo	bulk-seq
25	Insensitive	Melanoma	$BRAF^{amp}$	De-novo	bulk-seq
28	Insensitive	Melanoma	$PTEN^{Y88*}$	De-novo	bulk-seq

Abbreviations: CN, copy number; AF, allele frequency.
Additional alterations identified in the PDX are shown in Fig. 4d and Supplemental files.
BTK^{R46H} AF: 0 (PDX7), 0.05 (PDX7-EiR p0), 0.1(PDX7-EiR p1)
BRAF CN: see Fig. 4e (PDX1D and PDX1E); 5 (PDX25)

Supplementary Table II. Characteristics of patients treated with ERK signaling inhibitors

Patient	Sex	Cancer	Stage	Chemotherapy	RAFi	MEKi	ERKi
A	F	Glioblastoma	IV	Temozolamide	na	na	BVD523
B	F	NSCLC	IV	Carbo/Pem	na	na	BVD523
C	M	Melanoma	IV	na	Dabrafenib	Trametinib	BVD523
D	M	Melanoma	IV	na	Dabrafenib	Trametinib	BVD523
E	F	Melanoma	IV	na	Dabrafenib	Trametinib	BVD523
F	M	NSCLC	IV	Pem/Bev	Dabrafenib	Cobimetinib	na
G	M	NSCLC	IV	Pem/Bev	Dabrafenib	Trametinib	na
H	M	NSCLC	IV	Carbo/Pem/Doce	Vemurafenib	Trametinib	na
I	M	NSCLC	IV	Cis/Pem/Bev	Vemurafenib	Trametinib	na

Abbreviations: NSCLC, non-small cell lung cancer; Carbo, carboplatin; Pem, pemetrexed; Doce, docetaxel; Bev, bevacizumab; na, not applicable.

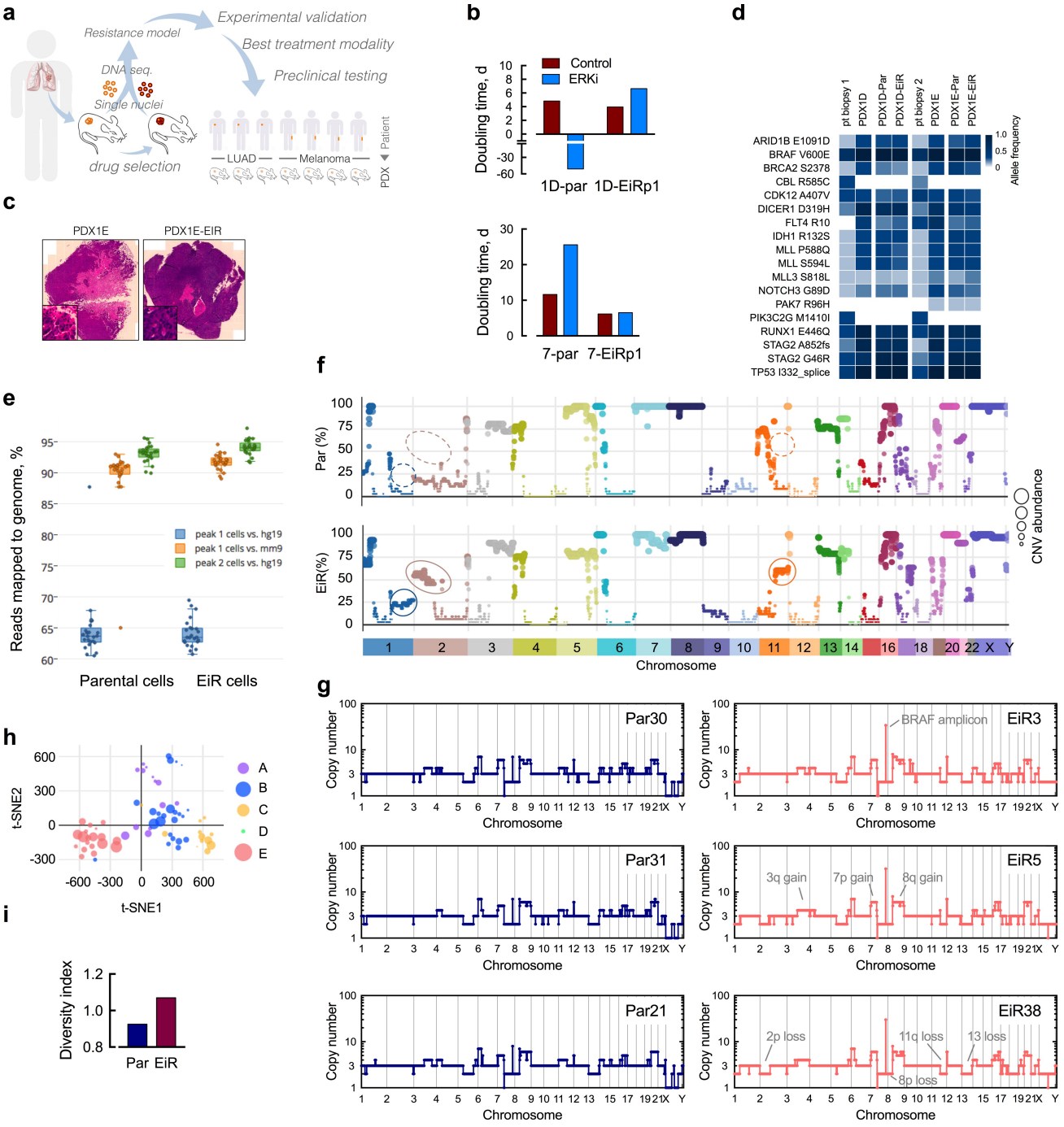

Supplementary Figure 1: Characterization of ERK inhibitor-resistant PDX models. (**a**) Schematic of this study's approach. Pairs of isogenic BRAF^{V600E}-mutant lung cancer PDX were used to establish the pattern by which resistance evolves at the single cell level. We then experimentally derived a model to explain this process and validated the effect of therapies predicted by the model in a panel of lung and melanoma PDX.-(**b**) The parental PDX models shown, or their derivatives that grew in the presence of ERKi, were treated with the drug to determine the effect on doubling time (n = 5 mice, mean). Par: parental, EiR: ERK-inhibitor resistant, p: passages in athymic mice. (**c**) H&E stained sections of the PDX models before and after ERKi treatment. (**d**) Proportion of single nucleotide variants (SNV) identified in biopsies and xenografts derived from patient 1. (**e**) Genomic DNA extracted from near-diploid (peak 1) or polyploid (peak 2) nuclei was amplified and subjected to sparse massively parallel sequencing. Sequencing reads were mapped to reference human or mouse genomes, revealing the presence of triploid human tumors supported by diploid mouse stroma. (**f**) The abundance of copy number variations (CNV) in the indicated chromosomal regions in single cells derived from parental or EiR tumors. Segment amplification (integer CN>3) or deletion (integer CN<3) were counted as individual CNV events. (**g**) CN profiles of representative parental (blue) and EiR (red) single cells. (**h**) t-Distributed Stochastic Neighbor Embedding (t-SNE) analysis of single cells showing the subclonal distribution. (**i**) Shannon diversity index analysis of Par and EiR tumors.

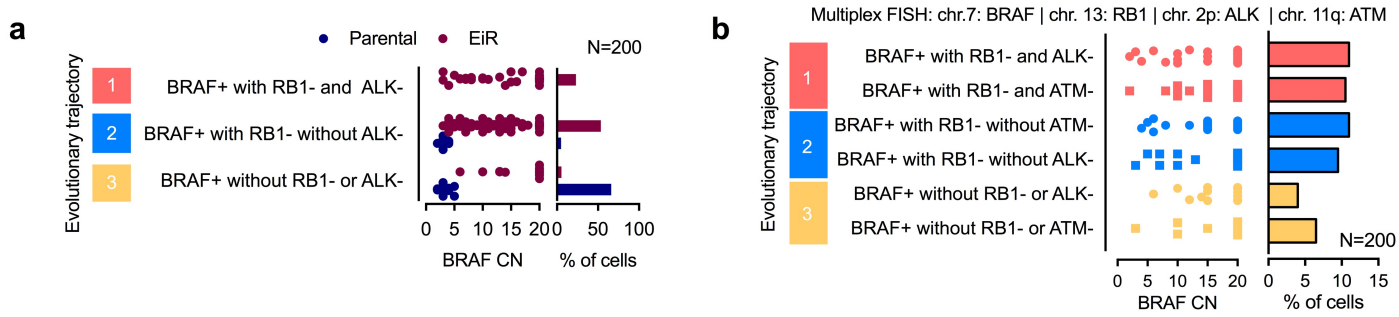

Supplementary Figure 2: Clonal structure of parental and ERK inhibitor resistant tumors. Multiplex FISH with probes targeting the indicated chromosomal regions in PDX1D and 1D-EiR cells (**a**) or in PDX1E-EiR, an ERK inhibitor-resistant model derived independently of PDX1D-EiR (**b**). Because the CN losses in chromosome 2p and 11q occur together, FISH probes detecting *BRAF/RB/ALK* or *BRAF/RB/ATM* constitute orthogonal approaches to validate the presence of distinct $BRAF^{amp}$ subclones.

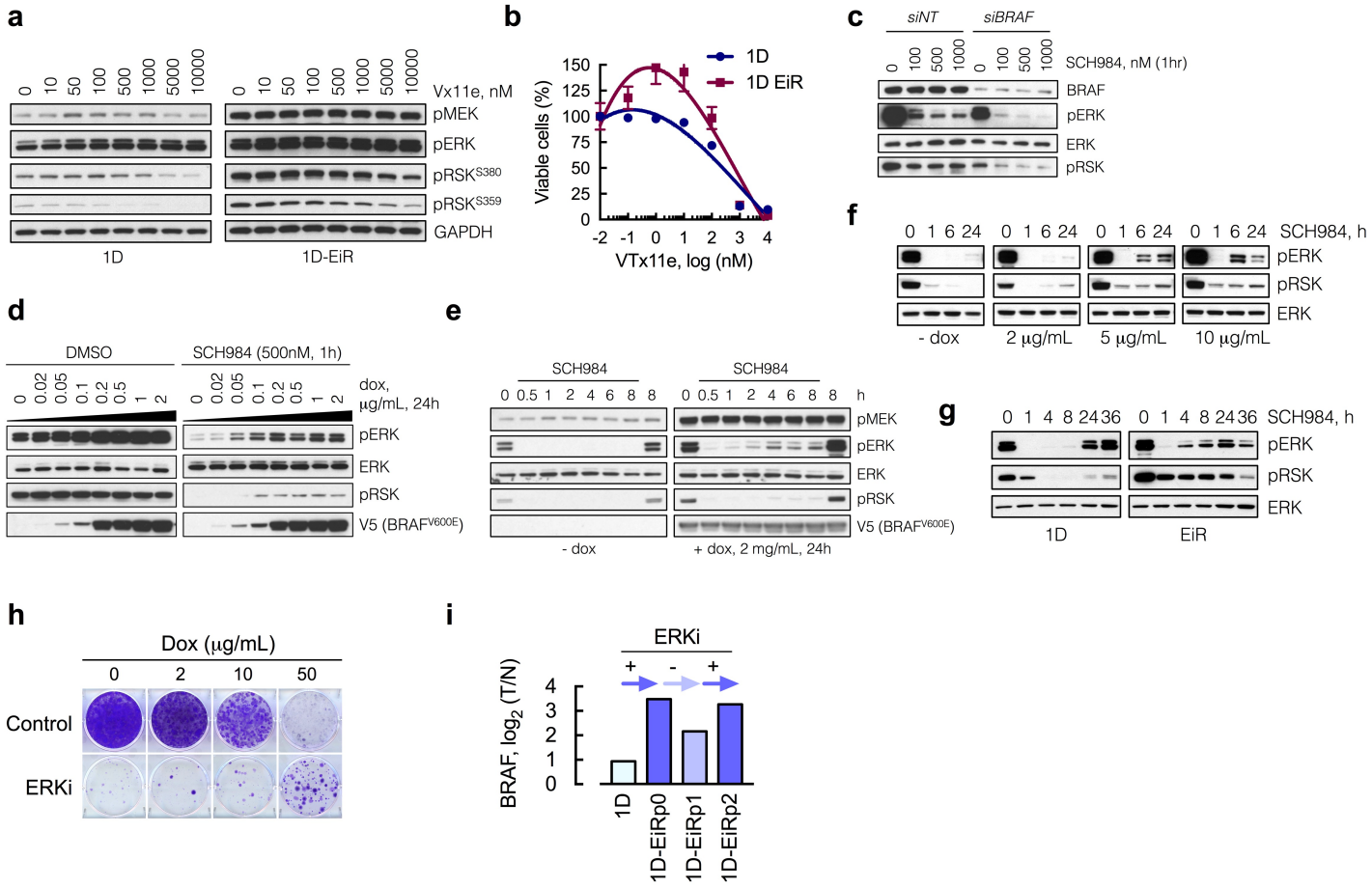

Supplementary Figure 3: Increased expression of BRAF^{V600E} diminishes the sensitivity to ERK inhibitors. (**a**) Immunoblot analysis of 1D and 1D-EiR cells treated with VTx11e for 1h. Unlike SCH984, VTx11e does not inhibit the phosphorylation of ERK. (**b**) Viability of cells treated for 72h with VTx11e (n = 3, mean ± s.e.m). (**c**) Immunoblot analysis of 1D-EiR cells transfected with BRAF specific or non-targeting siRNAs followed by drug treatment. (**d-f**) Immunoblot analysis of A375 cells engineered to express BRAF^{V600E}- under a doxycycline (dox)-induced promoter stimulated with increasing concentrations of dox (d), followed by treatment with the ERKi for the indicated times (e, f). (**g**) Immunoblot analysis of 1D and EiR cells treated with SCH984 (500 nM) as shown to determine pathway adaptation to the drug. (**h**) Clonogenic assay of A375 cells grown in various concentrations of dox and treated with or without the ERKi (SCH984, 500 nM) . (**i**) The *BRAF* CN of PDX 1D and PDX 1D-EiR passaged in the presence or absence of ERKi treatment determined by targeted next generation sequencing. At least two independent experiments were performed for all immunoblots shown in this figure.

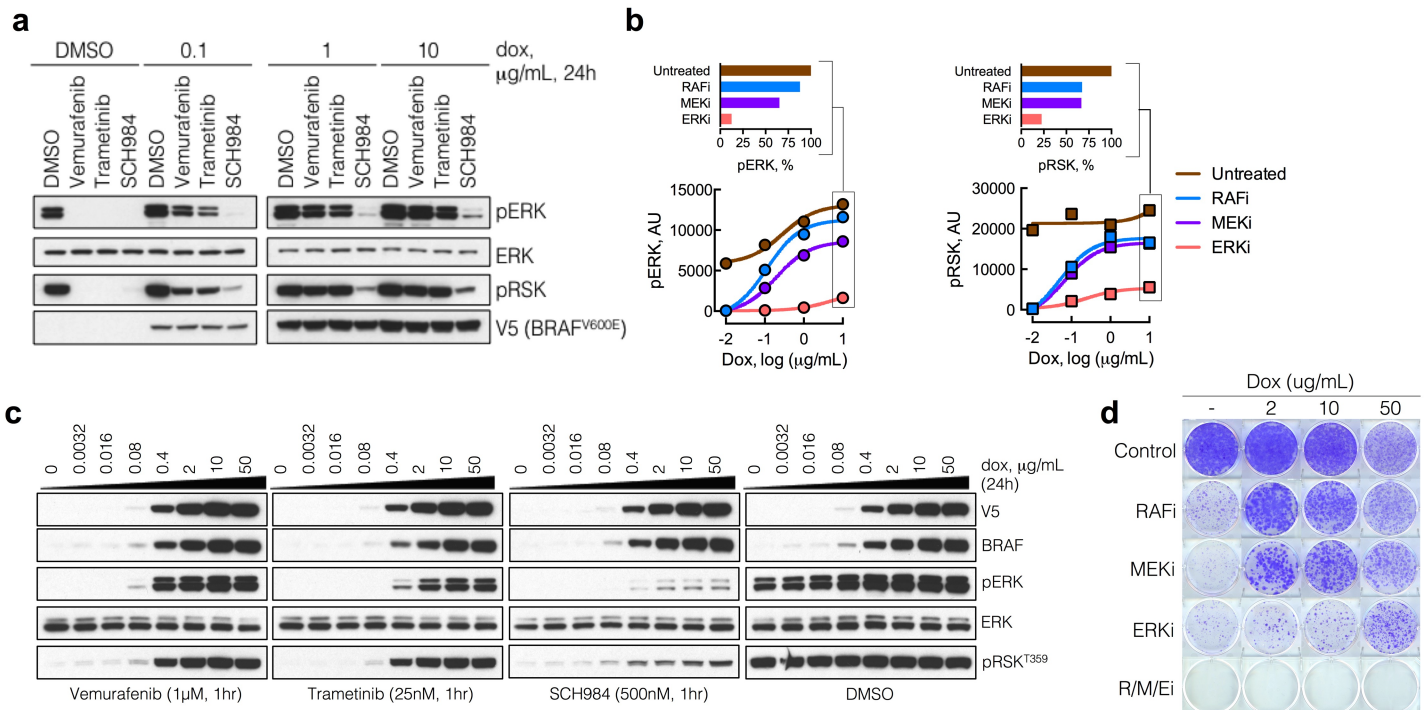

Supplementary Figure 4: A different level of BRAF^{V600E} expression is required to bypass the effect of distinct ERK signaling inhibitors. (a-c) Dox-stimulated A375 cells were treated for 1h with inhibitors of ERK signaling (doses as in Fig. 4b) to determine the effect of BRAF^{V600E} expression on the inhibition of ERK signaling intermediates. Representative immunoblot images from 2 independent experiments are shown (a, c). Quantification of (a) by densitometry (b). (**d**) Representative clonogenic assay of A375 cells grown in various concentrations of dox and treated as indicated (n = 2 independent experiments).

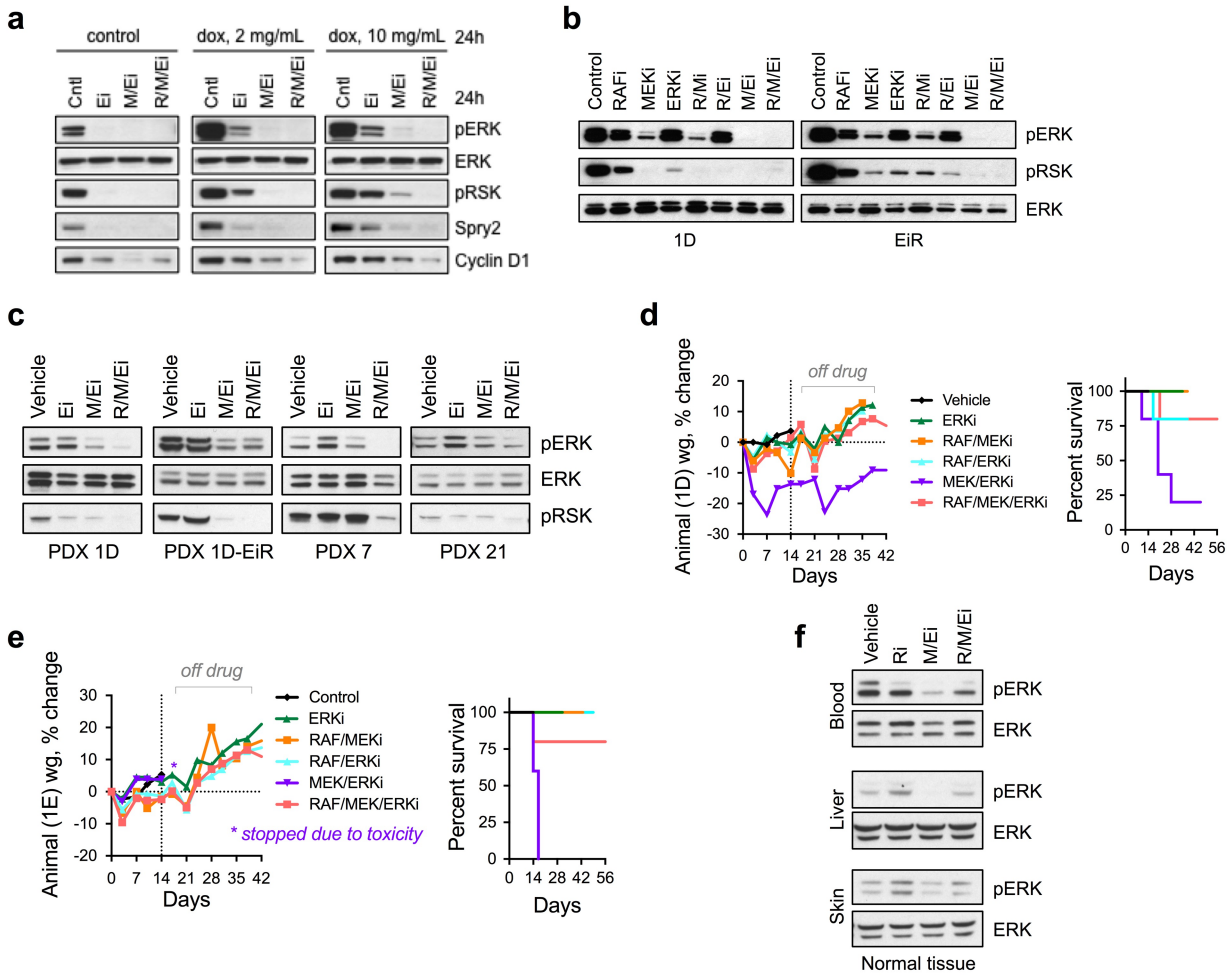

Supplementary Figure 5: Antitumor and toxicity profile of combination treatments utilizing ERK signaling inhibitors. (**a**) Immunoblot analysis (n = 2 independent experiments) of dox-stimulated A375 cells treated for 24h with an ERKi alone or in combination with RAF and/or MEKi, at the concentrations described in Fig. 5a. (**b**) Immunoblot analysis of 1D and 1D-EiR cells treated for 24h. (**c**) Immunoblot analysis of tumor cell extracts from PDX models treated for 24h as shown. (**d**, **e**) The effect of multidrug treatments on the weight and survival of mice bearing PDX1D or 1E (n = 5 mice). (**f**) Immunoblot analysis of cell extracts from various organs of mice treated with the indicated drugs.

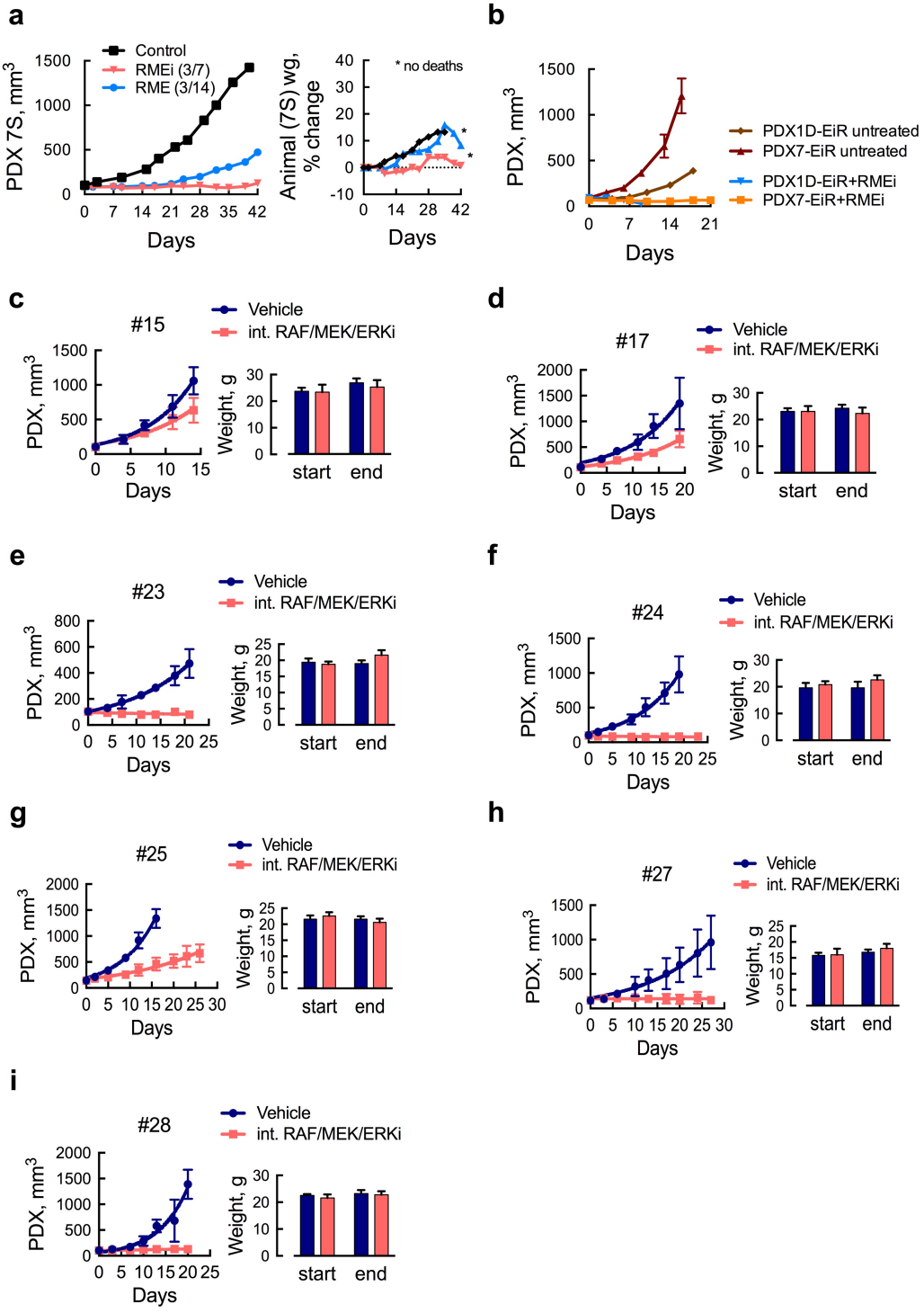

Supplementary Figure 6: The effect of the intermittent combination therapy on lung cancer and melanoma BRAF^{V600E} PDX models. (**a-i**) Mice bearing the indicated tumors were treated with RAF, MEK and ERKi to determine the effect on tumor growth and animal weight. (**a**) Optimization of the three-drug intermittent administration scheme. (**b**) The effect of treatment in models with acquired resistance to the ERKi. (**c**, **d**) PDX models harboring BRAF^{WT}. (**e-i**) PDX models derived from patients with BRAF^{V600E}-mutant melanoma. The weight at the onset and termination of treatment is shown. No deaths were observed during treatment. For all panels, n = 5, mean ± s.e.m; p: unpaired two-tailed t test between MEK/ERKi and int. RAF/MEK/ERKi-treated tumors.

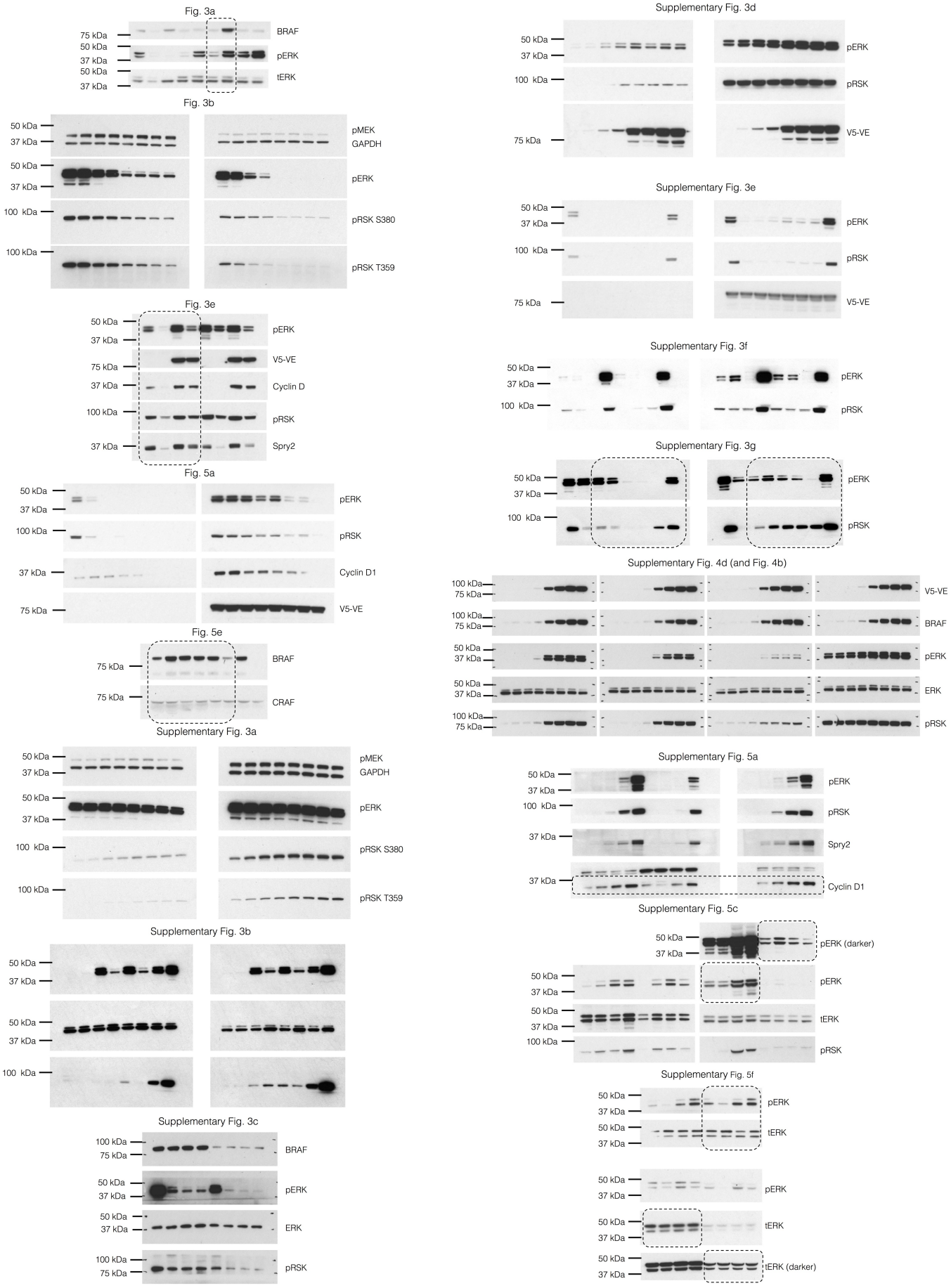

Supplementary Figure 7: Original images of representative immunoblots with molecular weight standards.